to 37,940) of the genome, which represents the actual coding sequence, was generated the pattern did not show similarity to those of the coding sequences in the first 20,000 bases of the genome (data not shown). Thus all the coding regions of the genome do not exhibit similar compositional bias.

The compositional heterogeneities of nucleotide sequences at isochore level were analysed by Karlin *et al.*[2] using dinucleotide relative abundance values, which assess the contrast between observed dinucleotide frequencies and those expected from the component mononucleotide frequencies. A differential map plotting such dinucleotide relative abundance values can be constructed following a formalism similar to that reported here. However, such differential maps will be statistically significant only for long contigs of DNA sequences (> 100 kb) and hence will not be suitable to analyse the local bias in sequences. This formalism may be extrapolated to map the trinucleotide frequencies of any sequence, in which the map will have sixty-four axes instead of sixteen.

It has already been reported that compositional analysis of nucleotide sequences can be used to address various problems such as discrimination between introns and exons of eukaryotic sequences[7], presence of local bias in dinucleotide compositions in regulatory regions of the genome (promoter, enhancer, etc.)[2], assessment of the coding potential of putative ORFs in uncharacterized DNA sequences, etc.[6]. However, all these studies involve a large number of numerical variables and the technique described here might be useful for simultaneous pictorial representation and visual comparison of such variables. Some of these problems are currently under study in our laboratory.

ACKNOWLEDGEMENTS. We gratefully acknowledge the valuable suggestions and constructive criticisms by Dr J. Das, Biophysics Division, IICB, Calcutta and Dr V. Nanjundiah of Developmental Biology and Genetics Laboratory of the Indian Institute of Science, Bangalore. C.D. is an Associate of Centre for Mathematical Modelling and Computer Simulation, National Aerospace Laboratories, Bangalore. A.P., S.B. and R.M. are respectively indebted to CSIR, DST and DBT, New Delhi for fellowships and associateships. Financial assistance by CSIR, UGC, DBT, New Delhi to D.P.B. and by DBT to C.D. is acknowledged.

Received 26 February 1996; revised accepted 21 May 1996.

1. Nussinov, R., *Nucleic Acids Res.*, 1980, **19**, 4545–4562.
2. Karlin, S., Ladunga, I. and Blaisdell, B. E., *Proc. Natl. Acad. Sci. USA*, 1994, **91**, 12837–12841.
3. Jeffrey, H. J., *Nucleic Acids Res.*, 1990, **18**, 2163–2170.
4. Dutta, C. and Das, J., *J. Mol. Biol.*, 1992, **228**, 715–719.
5. Karlin, S. and Campbell, A. M., *Proc. Natl. Acad. Sci. USA*, 1994, **91**, 12842–12846.
6. Borodovsky, M., Koonin, E. V. and Rudd, K. E., *Trends Biochem. Sci.*, 1994, **19**, 309–313.
7. Claverie, J. M., Sauvaget, I. and Bougueleret, L., *Methods Enzymol.*, 1990, **183**, 237–252.
8. Echols, H. and Goodman, M. F., *Annu. Rev. Biochem.*, 1991, **60**, 477–511.
9. Kunkel, T. A., *Bioessays*, 1992, **14**, 303–308.
10. Kreig, A. M., Yi, A-K., Matson, S., Waldschmidt, T. J., Bishop, G. A., Teasdale, R., Koretzky, G. A. and Klinman, D. M., *Nature*, 1995, **374**, 546–549.
11. Dickerson, R. E., *Methods Enzymol.*, 1992, **211**, 67–111.
12. Calladine, C. R. and Drew, H. R., in *Understanding DNA*, Academic Press, San Diego, 1992.
13. Peng, C. K., Bukdyrev, S. V., Goldberger, A. L., Havlin, S., Sciortine, F., Simons, M. and Stanley, H. E., *Nature*, 1992, **356**, 168–170.
14. Burma, P. K., Raj, A., Deb, J. K. and Brahmachari, S., *J. Biosci.*, 1992, **17**, 395–411.
15. Nandy, A., *Curr. Sci.*, 1994, **66**, 309–314.

Differences in energy metabolism in cells of neuronal and glial origin – ^{31}P NMR spectroscopic study

Archana Singh and Nanda B. Joshi

Department of Biophysics, National Institute of Mental Health and Neurosciences, Bangalore 560 029, India

^{31}P NMR spectroscopy has been used to study the energy metabolism in PC12 and U-87MG cells of neuronal and glial origin respectively. Both types of cells exhibited the resonances arising from adenosine triphosphate, inorganic phosphate and phosphomonoester. In addition, phosphocreatine was found to be present in PC12 cells whereas in U-87MG cells a prominent resonance due to diphosphodiester was observed. The pathways of ATP production were investigated using specific inhibitors of glycolysis and oxidative phosphorylation. Both glycolysis and oxidative phosphorylation pathways contribute to ATP production in PC12 cells, whereas oxidative phosphorylation was found to be the major ATP producing pathway in U-87MG cells. These results indicate that the energy-producing pathways in the cells of neuronal and glial origin could be different.

ADENOSINE TRIPHOSPHATE (ATP) serves as a primary currency of cells, fuelling cellular processes from macromolecular synthesis to signal transduction. It is well known that ATP production is tightly coupled to its consumption. The viability of cells depends on their energy utilization and it is probable that cell death, which is related to a breakdown in membrane function and/or inhibition in macromolecular synthesis, is produced by a local decrease of ATP below a critical level. This suggests that a large and unfavourable perturbation in the energy pathways could be responsible for an impaired cellular function. An impairment in the energy metabolic pathways of the affected cells or tissues has been observed in many neuronal disorders[1–6]. Very often, changes in the normal functioning of cells have been shown to be affected due to the alterations in the energy utilization pathways[7–11]. A detailed understanding of cel-

lular energy metabolism is, therefore, vital. NMR spectroscopy is ideally suited for investigating the cellular energy metabolism of intact cells[12–16]. ^{31}P NMR spectroscopy of cells provides quantitative information about the various phosphorylated metabolites produced in the energy production and utilization pathways. In addition, intracellular pH and phospholipid metabolism can be studied using ^{31}P NMR spectroscopy. In the present study, the energy metabolism in cells of neuronal (PC12) and glial (U-87MG) origin has been investigated using ^{31}P NMR spectroscopy.

Eagle's minimum essential medium (EMEM) and RPMI-1640 were purchased from Hi-media, Bombay (India). Foetal calf serum was obtained from Biological Industries, Israel. Bovine and horse serum were prepared in the laboratory. Sodium pyruvate, glutamine, glucose, N-2-hydroxy methyl piperazine-N-2 ethane sulfonic acid (HEPES), deuterium oxide (D_2O) and 2-deoxy-D-glucose (2-DG) were purchased from Sigma (USA) while sodium azide was obtained from Loba Chemei Indo Astranal Co., Bombay (India). All other chemicals were procured from various commercial sources and were of analytical grade.

PC12, a rat pheochromocytoma cell line, was obtained from National Tissue Culture Facility (NTCF), Pune (India) and U-87MG, a glioblastoma-astrocytoma cell line, was procured from American Type Culture Collection (ATCC), Rockville, MD (USA). Cells were grown in Nunc plastic tissue culture flasks or in glass bottles at 37°C under CO_2 environment. For PC12 cells, the growth medium consisted of RPMI-1640 with 10% horse serum, 5% foetal calf serum, 20 mM Hepes, 2 mM glutamine, 10 mM sodium bicarbonate and antibiotics. The growth medium for U-87MG cells consisted of EMEM with 5% foetal calf serum, 5% bovine serum, 10 mM Hepes, 1 mM sodium pyruvate and antibiotics. The cells were harvested at 120 h, centrifuged at 1500 rpm for 10 min and resuspended in HBSS containing glucose.

Cells were embedded in an agarose gel matrix in the form of threads so that the cells were held stationary in the NMR tube. Cell embedded gel threads were prepared by the method of Lyon *et al.*[17]. Briefly a solution of low gelling temperature agarose (2.6% w/v) was prepared in Hank's balanced salts solution (HBSS) at 50°C. Subsequently, the agarose solution was cooled to 37°C and 1 ml of this solution was mixed with 1 ml of cell suspension so that a typical sample contained 200×10^6 cells/ml. The gel matrix was then extruded under mild pressure through a coil of teflon tubing (0.5 mm i.d.) chilled in an ice-water bath at 10°C. The cell embedded gel threads were collected directly into 1 ml HBSS at the bottom of a 10 mm NMR tube. The 10 mm Wilmad screw cap NMR tube was modified to allow the perfusion of cells. A perfusion insert was fabricated with an inlet and outlet tubing. The insert was fixed on top of the NMR tube after the gel threads were collected. The cells embedded in the gel threads were perfused with balanced salt solution using a peristaltic pump with a flow rate of 1 ml/min.

^{31}P NMR measurements were performed on a Bruker AMX-400 NMR spectrometer with wide bore using 10 mm broad band probe. Spectra were acquired with a field frequency D_2O lock and without proton decoupling. Magnetic field homogeneity was adjusted by maximizing the D_2O free induction decay. ^{31}P NMR spectra were obtained at 161.98 MHz using a 15 µs excitation pulse and 1 sec delay time. Chemical shift was measured relative to phosphoric acid and the measurements were performed at 22°C. ^{31}P NMR experiments have been performed 3–5 times for both PC12 and U-87MG cells from different passages. The results were reproducible, however, the ^{31}P NMR spectra shown in Figure 1 are from typical experiments.

Cell viability was measured using trypan blue dye exclusion method after embedding the cells in the agarose gel threads and again after the NMR experiments were completed. 90–95% cells were found viable at the end of the NMR experiments. This clearly indicates that the cells were metabolically active during the NMR measurements.

Figure 1 shows the ^{31}P NMR spectra of PC12 and U-87MG cells from typical experiments. Both PC12 and U-87MG cells showed resonances arising from ATP, P_i and phosphomonoesters (PME). PC12 cells also showed a resonance due to phosphocreatine (PCr) which was absent in U-87MG cells. On the other hand, U-87MG cells showed a pronounced resonance due to diphosphodiesters (DPDE), which was relatively small in PC12 cells. Since PCr is produced by the enzymatic reaction involving creatine kinase (CK), it is probable that the

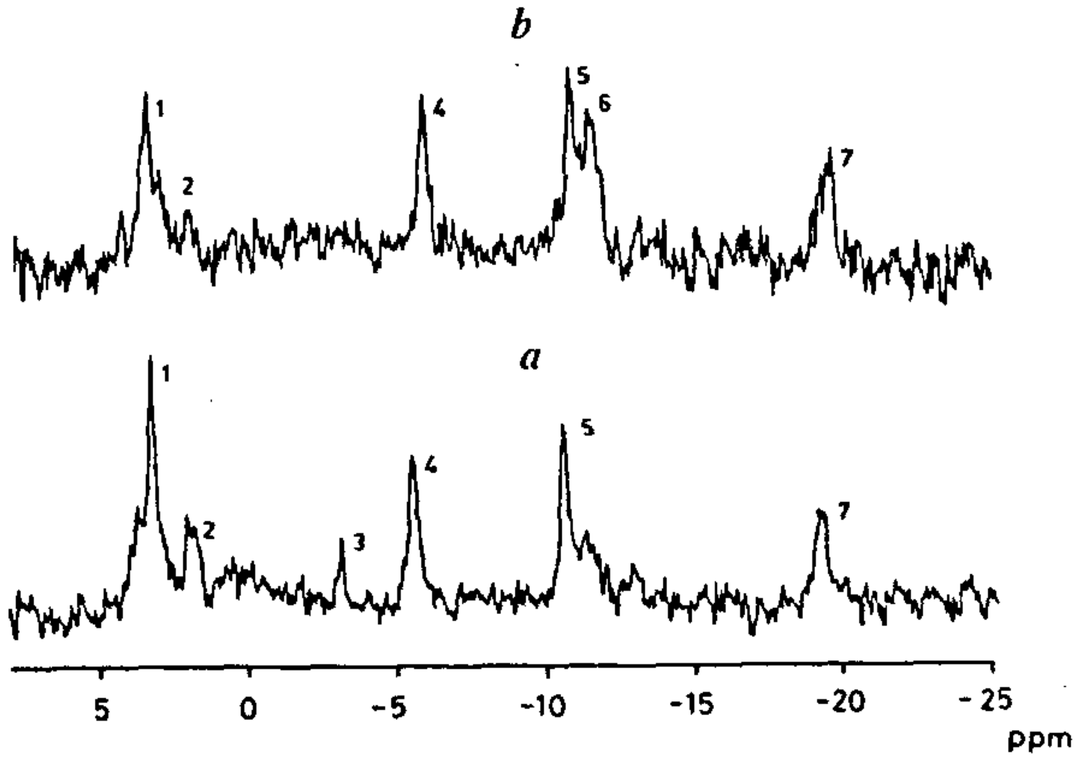

Figure 1. ^{31}P NMR spectra of PC12 and U-87MG cells embedded in agarose gel threads and perfused with HBSS containing glucose during the NMR experiments. *a*, PC12 cells and, *b*, U-87MG cells. Spectra were collected 1 h after casting the gel threads. Peaks are assigned as: (1) PME; (2) P_i; (3) PCr; (4) γ-ATP; (5) α-ATP; (6) DPDE and (7) β-ATP.

absence of PCr signal in ^{31}P NMR spectrum of U-87MG cells could be due to the impaired CK activity in these cells. It is also possible that PCr may be present in U-87MG cells in the bound form and therefore is inaccessible to the detection by NMR technique. Holtzmann *et al.*[18] have proposed that in the brain PCr is present in at least two different compartments, one is labile and thought to be present in neuronal cells and the other is stable and is present in astrocytes. The DPDE resonance observed in ^{31}P NMR spectra may arise from the uridine-diphosphosugars, in particular from uridine diphosphoglucose (UDPG). When glucose enters the cells, it may be metabolized to yield energy or it may be stored as an energy reserve in the form of glycogen. The synthesis of glycogen involves the formation of UDPG. The DPDE peak observed in ^{31}P NMR spectrum of U-87MG cells indicates the presence of glycogen reserves in these cells. Glycogen granules are known to be characteristic of astrocytes[19]. The PME peak, which was observed in both the cell types, may arise from phosphoethanolamine, phosphocholine and sugar phosphates in the cells[15].

The peak positions of ATP and P_i were almost the same in both types of cells. The same position of P_i (1.9 ppm) in both types of cells suggests that the intracellular pH of these cells is almost similar. The intracellular pH was calculated using the equation[11].

$$pH_i = 6.66 + \log(P_i - 3.079)/(5.57 - P_i)\,,$$

where P_i is the chemical shift of the inorganic phosphate peak relative to PCr peak. The pH_i of PC12 cells, thus calculated, was found to be 7.38. We could not calculate the pH_i in case of U-87MG cells as the PCr peak was not observed in these cells.

To determine the pathways of ATP production, the cells were perfused with the medium containing sodium azide and 2-deoxy-D-glucose (2-DG) during the NMR measurements. Sodium azide is an inhibitor of oxidative phosphorylation and prevents the production of ATP by blocking cytochrome oxidase, the last step in the electron transport chain. On the other hand, 2-DG blocks the glucose metabolism and inhibits the ATP production by glycolysis. On perfusing PC12 cells with the medium containing sodium azide, the PCr peak disappeared and a partial decrease in ATP was observed. However, on perfusing U-87MG cells with the medium containing sodium azide, a significant inhibition in ATP peaks was observed. Perfusion of PC12 cells with the medium containing 2-DG caused the appearance of 2-deoxy-D-glucose-6-phosphate (2-DG6P) with a complete inhibition of ATP peaks. U-87MG cells showed a small decrease in ATP signal on perfusing with the medium containing 2-DG, and an additional peak due to 2-DG6P was observed. These results are shown in Table 1 in terms of the ratio of P_i and β-ATP (P_i/β-ATP). In presence of NaN_3 in the perfusion medium, no appreciable change in the ratio of P_i/β-ATP was observed in PC12 cells while U-87MG cells showed an increase in P_i/β-ATP ratio. On addition of 2-DG to the perfusion medium the P_i/β-ATP ratio showed no change in U-87MG cells, however, in PC12 cells an increase in the same was observed. In PC12 cells, the inability of sodium azide to inhibit the ATP peaks indicates that glycolysis also contributes to ATP generation. This is further confirmed by inhibition of ATP peaks in the presence of 2-DG. Thus in PC12 cells, ATP is generated by both glycolysis and oxidative phosphorylation. On the other hand, in U-87MG cells, a significant inhibition of ATP by sodium azide and no further inhibition by 2-DG suggest that oxidative phosphorylation is the major pathway of ATP production.

Table 1. The ratio of inorganic phosphate (P_i) and adenosine triphosphate (β-ATP) *in PC12 and U-87MG cells perfused with HBSS*

Perfusion medium	P_i/β-ATP	
	PC12 cells	U-87MG cells
HBSS + glucose	0.80 ± 0.15	0.33 ± 0.09
HBSS + glucose + NaN_3	0.97 ± 0.30	4.10 ± 0.54
HBSS + glucose + NaN_3 + 2DG	21.80 ± 1.83	4.27 ± 0.53

Cells were embedded in agarose gel threads and were perfused with HBSS during the NMR measurements. NaN_3 or NaN_3 + 2DG were added to the perfusate one hour before starting the experiments and were present during the data collection. P_i/β-ATP ratio given is the mean ± SE of three experiments.

The present study has shown that the cells of neuronal and glial origin have some differences in their energy metabolic pathways. These cells appear to differ in their energy metabolism and the differences in the cellular energy metabolism may probably be due to their specialized functional role.

1. Beal, M. F., *Ann. Neurol.*, 1992, **31**, 119–130.
2. Beal, M. F., Hyman, B. T. and Korostz, W., *Trends Neuro Sci.*, 1993, **16**, 125–131.
3. Calabrese, G., Deicken, R. F., Fein, G., Merrin, E. L., Schoenfeld, F. and Weiner, M. W., *Biol. Psychiatry*, 1992, **32**, 26–32.
4. Pettegrew, J. W., *Annu. N. Y. Acad. Sci.*, 1989, **568**, 5–28.
5. Evanochko, W. T., Ng, T. C. and Glickson, J. D., *Mag. Reson. Med.*, 1984, **1**, 508–534.
6. Lees, G. J., *Neuroscience*, 1993, **54**, 287–322.
7. Ben-Yoseph, O., Bachelard, H. S., Badar-Goffer, R. S., Dolin, S. J. and Morris, P. G., *J. Neurochem.*, 1990, **55**, 1446–1449.
8. Espanol, M. T., Yan Xu Litt, L., Yang, G. Y., Chang, L. H., James, T. L., Weinstein, P. and Chan, P. H., *J. Cerebral Blood Flow Metabol.*, 1994, **14**, 269–278.
9. Novelli, A., Reilly, J. A., Lysko, P. G. and Henneberry, R. C., *Brain Res.*, 1988, **451**, 205–212.
10. Storey, E., Hymann, B. T., Jenkins, B., Brouillet, E., Miller, J. M., Rosen, B. R. and Beal, M. F., *J. Neurochem.*, 1992, **58**, 1975–1978.
11. Decorps, M., Lebas, J. L., Leviel, J. L., Confort, S., Remy, C. and Benabid, A. L., *FEBS Lett.*, 1989, **168**, 1–6.
12. Weiner, M. W., *Investigative Radiol.*, 1988, **23**, 253–261.

13. Radda, G. K., *FASEB J.*, 1992, **6**, 3032–3038.
14. Bachelard, H. and Badar-Goffer, R., *J. Neurochem.*, 1993, **61**, 412–429.
15. Cohen, J., *Mayo Clin. Proc.*, 1988, 1199–1207.
16. Foxall, D. L. and Cohen, J. S., *J. Magn. Reson.*, 1983, **52**, 346–349.
17. Lyon, R. C., Faustino, P. J. and Cohen, J. S., *Magnetic Reson. Med.*, 1986, **3**, 663–672.
18. Holtzmann, D., McFarland, E., Moerland, T., Koutcher, J., Kushmerick, M. J. and Neuringer, L. J., *Brain Res.*, 1989, **483**, 68–77.
19. Roots, B. I., in *Dynamic Properties of Glial Cells* (eds Schoffenils, E., Frank, G., Towers, D. B. and Hertz, L.), Pergamon Press, Oxford, 1978, p. 50.

ACKNOWLEDGEMENT. The NMR experiments were performed at the Sophisticated Instruments Facility, Indian Institute of Science, Bangalore.

Received 7 February 1996; revised accepted 14 May 1996

Anomalous helium emission: Precursor to earthquakes

Debasis Ghose, Nishith Kr. Das and Bikash Sinha

Variable Energy Cyclotron Centre, Department of Atomic Energy, 1/AF Bidhan Nagar, Calcutta 700 064, India

Helium content at the thermal springs at Bakreswar, near Calcutta, was observed to vary. These variations appear correlated to seismic perturbations. The position and distance of epicentre cannot yet be predicted from such correlation.

THERE is adequate evidence that the variations in the relative abundance of the constituents of terrestrial gas have certain degree of correlation with the perturbations within the mantle as well as the crust of earth[1]. A recent report has indicated that there was a ten-fold increase in the radon content in bore hole gas prior to the earthquake at Kobe, Japan[2]. Anomalously high helium concentrations have also been reportedly observed in well waters and soil gases preceding an earthquake[3,4].

It is well established by now that noble gas such as helium and radon interact weakly with matter; thus, it is expected that there will be pronounced variations in their relative abundance for such perturbations just mentioned, compared to their chemically reactive counterparts, such as nitrogen and methane. In the case of radon on account of chemical non-equilibrium and short recoil length, the host rocks incorporating the parent Ra-226 migrates rather large distances in water and in soil[5]. However, its relatively short decay time (3.82 days) inhibits any substantial concentration, so that very marginal radon content contribute above background value[6]. Over the last several years, we have been observing large fluctuation in helium concentration in the natural gas emanating from thermal springs[7]. Three mechanisms have been suggested so far to account for the anomalies observed for the constituents of the soil gas in seismic-induced disturbances: (i) relative increase in heat flow that enhances gas concentrations near the surface[7,8], (ii) stress-induced pore collapse resulting in an upward flow of deep-seated gas[9]. (iii) stress-induced microfracturing leading to an increase in outgassing[10]. The collected sample of natural gas issuing from thermal springs was measured analytically by two separate techniques. A gas chromatograph operational at Bakreswar, the site of investigation (about 200 kms from Calcutta), of Variable Energy Cyclotron Centre was used to determine the relative abundances of helium and associated gases. Furthermore, the relative abundance of helium was determined by an absolute method based on the technique first developed by Frost[11].

We found the helium abundance at Bakreswar to be a variable quantity in general. The computed average of helium abundance, taken from recorded data of the diurnal readings for a five-year period, 1987–1991 was around 1.8%. We call this the characteristic 'helium index' for the spring. The normal value of the emanation rate during the quiescent state was close to the above figure with approximately $\pm 0.2\%$ variation. However it had been observed that the index began to fall very gradually two to three weeks prior to an impending seismic disturbance, known as earthquakes. The index tended to reach the minimum value four to five days before the triggering of the quake. This scenario was immediately followed by a sharp rise in the index, reaching its highest value two to three days prior to the occurrence of the quake, the peak value being two to three times the minimum value. Indeed, the helium content increased to 7.3% immediately prior to the volcanic eruption at Barren Island in July 1991 (ref. 12).

The measured magnitude of the helium concentration at Bakreswar for October in 1991 is plotted in Figure 1; corresponding data for January in 1992 is in Figure 2 and for the subsequent month of April 1992 is shown in Figure 3.

It was generally seen that the profiles had an irregular oscillatory pattern. This is expected since the helium contained in any underground environment is at best in a fragile state of equilibrium. It should also be mentioned that the presence of other diluting gases such as N_2 and CH_4 affected very feebly the outflow of helium as observed by Reimer[4] in soil gas. For large scale deviations ($d > 3\sigma$) one has to thus look for catastrophic causes such as earthquakes as suggested by Scholz *et al.*[13]. In order to judge the long term and background behaviour of helium changes, emission graphs for the period June 1991 to October 1991, January 1992 to July 1992 and January 1993 to October 1993 (Figures 4–6) are given. The spring gas was collected